Novel Fe(III), Co(III), Ni(II), Cu(II) coordination compounds involving 2-[(2-hydroxyphenyl)methylene]hydrazine-N-(2-propenyl)-carbothioamide as ligand: Synthesis, crystal structur...

ARTICLE *in* INORGANICA CHIMICA ACTA · NOVEMBER 2014

Impact Factor: 2.05 · DOI: 10.1016/j.ica.2014.08.056

9 AUTHORS, INCLUDING:

Svitlana Orysyk
National Academy of Sciences of Ukraine
32 PUBLICATIONS **69** CITATIONS
SEE PROFILE

Hlib Repich
Institute of General and Inorganic Chemistry
3 PUBLICATIONS **1** CITATION
SEE PROFILE

Volodymyr Bon
Technische Universität Dresden
79 PUBLICATIONS **589** CITATIONS
SEE PROFILE

Oleg V Shishkin
National Academy of Sciences of Ukraine
837 PUBLICATIONS **4,819** CITATIONS
SEE PROFILE

Inorganica Chimica Acta 423 (2014) 496–503

Contents lists available at ScienceDirect

Inorganica Chimica Acta

journal homepage: www.elsevier.com/locate/ica

Novel Fe(III), Co(III), Ni(II), Cu(II) coordination compounds involving 2-[(2-hydroxyphenyl)methylene]hydrazine-N-(2-propenyl)-carbothioamide as ligand: Synthesis, crystal structures and spectral characteristics

S.I. Orysyk [a,*], G.G. Repich [a], V.V. Bon [b], V.V. Dyakonenko [d], V.V. Orysyk [c], Yu.L. Zborovskii [c], O.V. Shishkin [d,e], V.I. Pekhnyo [a], M.V. Vovk [c]

[a] V.I. Vernadskii Institute of General and Inorganic Chemistry, National Academy of Sciences of Ukraine, Palladin av. 32/34, 03680 Kyiv, Ukraine
[b] Department of Inorganic Chemistry, Dresden University of Technology, Bergstrasse 66, 01069 Dresden, Germany
[c] Institute of Organic Chemistry, National Academy of Sciences of Ukraine, Murmaska str. 5, 02660 Kyiv, Ukraine
[d] SSI "Institute for Single Crystals", National Academy of Science of Ukraine, Lenina av. 60, 61001 Kharkiv, Ukraine
[e] Department of Inorganic Chemistry, V.N. Karazin Kharkiv National University, 4 Svobody sq., 61077 Kharkiv, Ukraine

ARTICLE INFO

Article history:
Received 29 April 2014
Received in revised form 15 August 2014
Accepted 18 August 2014
Available online 16 September 2014

Keywords:
3d metal complexes
X-ray diffraction study
Carbothioamide
Stability constant
X-ray photoelectron spectroscopy
MALDI-mass spectrum

ABSTRACT

Novel Cu(II), Fe(III), Co(III) and Ni(II) coordination compounds with a 2-[(2-hydroxyphenyl)methylene]hydrazine-N-(2-propenyl)carbothioamide have been synthesized and characterized by single crystal X-ray diffraction, IR, UV–Vis, ^{1}H, (^{13}C) NMR and X-ray photoelectron spectroscopy. The optimal conditions for the complexation reactions have been determined. Depending on synthesis conditions the ligand coordinates to the metal ion as a neutral molecule, monoanion or bianion mode forming complexes with composition $[Cu(H_2L)Cl]$ (**I**), $[Fe(H_2L)_2]NO_3$ (**II**), $[Co(H_2L)_2]Cl$ (**III**) and [Ni(HL)Py] (**IV**). The stability constants for the compounds **I**–**III** have been calculated. It has been found that the ligand molecules are coordinated in a tridentate manner by the sulfur, azomethine nitrogen and phenol oxygen in both thione (complexes **I**–**III**) or thiolic (complex **IV**) tautomeric forms.

1. Introduction

Thiosemicarbazones are well known as efficient complexing agents [1–4] that forms stable complex compounds with transition metal ions. Recent studies show an important role of the latter in metabolic processes of living organisms [5–7]. The ability of thiosemicarbazides to form a molecular complexes with proteins as well as to bind metal ions, which are in the active site of enzymes, allows them to be used as inhibitors of a number of metalloenzymes, such as xanthine oxidase [8], ribonucleotide diphosphate reductase [9], tyrosinase [10,11], urease [12].

The introduction of new nucleophilic reaction centers into thiosemicarbazones allows to obtain both new polydentate ligands and new mono-, bi- and polynuclear complex compounds [2,13]. This causes the urgency to identify the factors affecting the complexation and widens their practical application. Both thiosemicarbazones and their complex compounds with transition metals possess a high biological activity: anticancer [14–17], antiretroviral [18], antibacterial [19,20], fungicidal [6], and antiprotozoal [21–23]. It should be noted that the complexes have an advantage in comparison with the free ligands or inorganic salts. Preserving the same pharmacologic properties complex formation hinders hydrolysis in biological media, reduces the drugs toxicity and facilitates their penetration through cell membranes. Besides, it is known to use of thiosemicarbazones in analytical chemistry and for the selective extraction of metal ions from aqueous solutions of their salts [24–32].

In this work we used 2-[(2-hydroxyphenyl)methylene]hydrazine-N-(2-propenyl)carbothioamide (*HPMHPCTA*) as a chelating reagent for studying its interaction with Fe^{3+}, Co^{2+}, Ni^{2+} and Cu^{2+} ions, since they are known as a component of numerous enzymes. The interaction of this chelating agent with the above ions may be interesting for the simulation of the interaction of metal enzymes with their inhibitors. In addition, thiosemicarbazone contains allyl lipophilic moiety, which can have a significant effect on biological activity and extraction properties of complex compounds based on it.

* Corresponding author. Tel.: +380 44 4240511; fax: +380 44 4243070.
E-mail addresses: s_oryslend@mail.ru, orysyk@ionc.kiev.ua (S.I. Orysyk).

http://dx.doi.org/10.1016/j.ica.2014.08.056
0020-1693/

We had previously determined pH range, wherein HPMHPCTA may exist in thiol–thione equilibrium: thione form of thiosemicarbazone predominates at pH $\leqslant$ 4, there is an equal ratio of thiol and thione forms of ligand at pH 4–6, and its thiol form predominates at pH $\geqslant$ 8. This allowed us to obtain zinc complex with thione form of HPMHPCTA coordination [33]. In addition, the copper and palladium complexes have been synthesized in a neutral medium, here two HPMHPCTA ligands are coordinated simultaneously in thiol and thione tautomeric forms in the same compound [34,35]. In our recent work we found that pH affects not only the tautomerism of thiosemicarbazone, but also its cyclizability. Thus, in acidic media (at pH $\leqslant$ 0.5–1.0) complexation is accompanied by HPMHPCTA cyclization with the formation of tetrahydropyrimidine-2-(1H)-thionic ring [34]. Performing the reaction in the neutral medium leads to conversion of the ligand into triazole [36]. Therefore, the main challenge is to find the reaction conditions for obtaining phase pure desired products with the coordination of HPMHPCTA either in thiol or in thione tautomeric form.

2. Experimental

2.1. Materials and physical measurements

Initial reagents $CuCl_2{\cdot}2H_2O$, $Fe(NO_3)_3{\cdot}9H_2O$, $Co(NO_3)_2{\cdot}6H_2O$, $Ni(NO_3)_2{\cdot}6H_2O$ used for the synthesis of complexes **I–IV** and for analytical investigations were purchased from Merck.

Elemental analyses for carbon, hydrogen, nitrogen and sulfur were performed by Carlo Erba Elemental Analyzer Model 1106. The chlorine was measured by Shoniger method. The IR spectra were recorded on a Specord M80 in the range 4000–200 cm^{-1} in KBr pellets. Electronic spectra of DMF solutions of *HPMHPCTA* and its complexes ($10^{-4}/10^{-1}$ mol L^{-1}) were recorded on a Specord M40 spectrophotometer in the range 50 000–11 000 cm^{-1} (200–900 nm) using a 1 mm quartz cell. X-ray photoelectron spectra (XPS) were measured on an ES-2402 device using Mo Kα radiation. Samples were prepared as thin films from an acetone suspension on a 10 × 10 mm aluminum base plate.

^1H (^{13}C) NMR spectra were measured on a Bruker Avance DRX-400 spectrometer (400.00 (125.75) MHz) in DMSO-d6 solution using TMS as internal standard.

Sample of complex **III** was prepared for laser desorption mass analysis as follows: the laser desorption matrix material (12 mg of 3,5-dimethoxy-4-hydroxycinnamic (sinapinic) acid) was dissolved in 1 mL of water/acetonitrile solution 1:1 (v/v). The obtained solution was incubated during 10 min at 30 °C in ultrasonic bath up to the full dissolving of the acid. 10 μL of studied solution was added to the matrix solution in 1:1 ratio. Small aliquot of mixture was applied to the steel probe tips and dried. Mass analysis was performed on "Autoflex II" ("Bruker Daltonics", Germany) MALDI-TOF mass spectrometer with nitrogen laser (λ = 337 nm). Spectrum was obtained for the mass range 100 000–2000 a.m.u. in positive ion reflectrone registration mode by summing the data of 100 laser shots.

2.2. Single crystal X-ray diffraction

Crystal structures of complexes **I**–**IV** were determined by single crystal X-ray diffraction. The measurements were performed on Bruker SMART APEX2 diffractometer (Mo Kα radiation, graphite monochromator, λ = 0.71073 Å) at 173 K in the stream of cold nitrogen. The data were collected using ω- and φ-scans and integrated with SAINT program [37]. The obtained intensities were corrected for Lorentz, polarization and absorption using multi-scan technique in SADABS program [38]. All structures were solved by direct methods and refined by full matrix least-square method against F^2 using SHELXTL program package [39]. Positions of the hydrogen atoms were located from difference Fourier maps and refined using a riding model with $U_{iso}(H) = nU_{eq}$ of carrier non-hydrogen atom (n = 1.5 for methyl groups and water molecule and 1.2 for other H atoms). In the crystal structure of **II**, the positional disorder of nitrate anion is treated by refinement of each part with occupancy of 50%. Although resolved disorder, the final residual parameters of the model are still high that could be explained by poorly scattered crystal. Unfortunately after several tries it was not possible to get a better one. High residual electron density after the final refinement cycle is due to the disorder of nitrate anions positions that could not be split further using dataset with such quality. Hydrogen atoms, connected to O and N were located from difference Fourier map and refined without constraints. All other H atoms were put in idealized geometrical positions and refined as a "riding model" on the host atom. In the structure of **IV**, the disorder of the coordinated pyridine molecule was resolved by splitting of all atoms over two positions with 50% occupancy of each one. The two pyridine rings is rotated one relative to another creating dihedral angle of 68.6(1)°. Crystallographic data for all structures have been deposited in the Cambridge Crystallographic Data Centre. Copies of the data can be obtained free of charge by an application to the Director, CCDC, 12 Union Road, Cambridge CB2 1EZ, UK (Fax: +44 1223 336 033; E-Mail: deposite@ccdc.cam.ac.uk; internet: http://www.ccdc.a-c.uk). The crystallographic parameters and detailed experimental data are given in Table 1.

2.3. Synthesis of Fe(III), Co(II), Ni(II), Cu(II) complexes *I–IV*

The preparation of *HPMHPCTA* and its ^1H, ^{13}C NMR spectral characteristics were submitted in [34,40]. Since the UV–Vis spectrum of all complexes has been studied in ethanol solutions, in this work we present UV–Vis data of ligand in ethanol. IR data, ν, cm^{-1}: 3621 broadened absorption band of intermolecular hydrogen bond; 3399, ν(OH); 3167, ν(NH); 3100, ν(=CH); 3004, asymmetric vibrations $\nu(CH_2)_{allyl}$; 2943, ν(CH); 1655, 1638 d, ν(—C=C—)$_{allyl}$; 1620, 1600 d, ν(C=N); 1543, 1520 d, in-plane deformation vibrations δ(NH—CS—NH); 1483, 1464, 1428, 1406, phenolic ring vibrations ν(PhH); 1352, 1326, ν(CS); 1287 ν(—C—N—); 1219 $\nu(C{-}O)_{Ph}$; 1147, 1081, ν(NH—CS—NH); 1035, 1000, ν(N—N); 947, 935 d, 903, in-plane deformation vibrations δ(CH); 804, 761, 736, 648, out-of-plane deformation vibrations δ(CH); broadened 617, 574, 548, 524, 481, 465, deformation vibrations $\delta(CH)_{allyl}$.

UV–Vis data, ν, cm^{-1} (EtOH): 43 000 (621), 41 230 (450), 34 030 (860), 32 800 (964), 30 000 (1317), 28 720 (955).

2.3.1. Cu(H_2L)Cl complex (*I*)

42.7 mg of $CuCl_2{\cdot}2H_2O$ (0.250 mmol) were dissolved in 20 mL of EtOH under heating. To the resulting solution was added a hot *HPMHPCTA* solution (58.7 mg, 0.250 mmol in 20 mL of EtOH) under constant stirring. The resulting green solution was boiled for 15 min, after which it was left for crystallization. After 3–4 days, brown–red crystals formed at the bottom of the vessel, which were filtered off and washed with alcohol and diethyl ether.

Decomposition temperature (dec.*t.*) 165 °C. Yield 0.059 g (71%). *Anal.* Calc. for $C_{11}H_{12}N_3SOCuCl$: C, 39.64; H, 3.63; Cl, 10.64; N, 12.61; S, 9.62. Found: C, 39.55; H, 3.68; Cl, 10.32; N, 12.77; S, 9.59%.

IR data, ν, cm^{-1}: 3621 broadened absorption band of intermolecular hydrogen bond; 3470, intramolecular hydrogen bond; 3281, ν(NH); 3063, ν(=CH); 2993, asymmetric vibrations $\nu(CH_2)_{allyl}$; 2777, ν(CH); 1656, ν(—C=C—)$_{allyl}$; 1600 ν(C=N); 1537, in-plane deformation vibrations δ(NH—CS—NH); 1466, 1449, 1430, 1405, phenolic ring vibrations ν(PhH); 1356, ν(CS); 1339, 1328, ν(—C—N—); 1202 $\nu(C{-}O)_{Ph}$; 1156, 1087, ν(NH—CS—NH); 1037, 1002, ν(N—N); 937, 908 in-plane deformation vibrations δ(CH);

Table 1
X-ray crystallographic experimental data for investigated compounds.

Compound	Complex **I**	Complex **II**	Complex **III**	Complex **IV**
Empirical formula	$C_{11}H_{14}ClCuN_3O_2S$	$C_{22}H_{24}FeN_7O_5S_2$	$C_{24}H_{30}ClCoN_6O_3S_2$	$C_{16}H_{16}N_4NiOS$
Formula weight	351.30	586.45	609.04	371.10
Crystal system, space group	triclinic, $P\bar{1}$	triclinic, $P\bar{1}$	triclinic, $P\bar{1}$	monoclinic, $P2_1/c$
Unit cell dimensions				
a (Å)	8.5533(4)	9.3717(8)	8.812(2)	4.9771(4)
b (Å)	8.9987(4)	11.7871(10)	12.192(3)	14.8027(9)
c (Å)	9.5524(4)	12.6102(14)	12.447(3)	21.2724(17)
α (°)	92.292(2)	73.025(6)	87.543(4)	
β (°)	108.810(2)	81.830(6)	82.371(5)	93.893(3)
γ (°)	98.182(2)	79.000(5)	86.872(5)	
Volume (Å^3)	685.98(5)	1302.3(2)	1322.6(5)	1563.6(2)
Z, D_{calc}(g cm^{-3})	2, 1.701	2, 1.496	2, 1.529	4, 1.576
μ (mm^{-1})	1.939	0.787	0.947	1.383
F(000)	358	606	632	768
Crystal size (mm)	0.47 × 0.13 × 0.09	0.07 × 0.046 × 0.02	0.5 × 0.4 × 0.3	0.63 × 0.15 × 0.14
θ range for data collection (°)	2.26–30.00	1.83–25.24	1.65–27.50	1.68–25.00
Limiting indices	$-12 \leqslant h \leqslant 12$, $-12 \leqslant k \leqslant 12$, $-13 \leqslant l \leqslant 13$	$-12 \leqslant h \leqslant 12$, $-12 \leqslant k \leqslant 15$, $-16 \leqslant l \leqslant 16$	$-11 \leqslant h \leqslant 11$, $-15 \leqslant k \leqslant 15$, $-16 \leqslant l \leqslant 16$	$-5 \leqslant h \leqslant 5$, $-17 \leqslant k \leqslant 16$, $-25 \leqslant l \leqslant 24$
Reflections collected/unique	14013/3929	15458/6433	14249/6058	11363/2742
Completeness to θ_{max} (%)	0.982	0.994	0.998	0.999
maximum/minimum transmission	0.8449/0.4627	0.984/0.947	0.769/0.658	0.8299/0.4737
Data/restrains/parameters	3929/0/172	6433/20/324	6058/7/337	2742/18/263
Goodness-of-fit (GOF) on F^2	1.031	1.094	0.860	1.059
Final R indices [$I > 2\sigma(I)$]	$R_1 = 0.0414$, $wR_2 = 0.0777$	$R_1 = 0.1317$, $wR_2 = 0.3340$	$R_1 = 0.0708$, $wR_2 = 0.1219$	$R_1 = 0.0238$, $wR_2 = 0.0574$
R indices (all data)	$R_1 = 0.0738$, $wR_2 = 0.0840$	$R_1 = 0.2932$, $wR_2 = 0.4262$	$R_1 = 0.1775$, $wR_2 = 0.1435$	$R_1 = 0.0315$, $wR_2 = 0.0600$
Largest difference in peak and hole (e Å^{-3})	0.396/−0.363	2.56/−0.81	0.828/−0.860	0.347/−0.314

808, 748, 728, 711 out-of-plane deformation vibrations δ(CH); broadened 634, 615, 551, 450 deformation vibrations $\delta(CH)_{allyl}$, 342, ν(Cu—N); 304 ν(Cu—Cl); 277 ν(Cu—S).

UV–Vis data, ν, cm^{-1} (EtOH): 40325 (911); 33745 (1077); 32707 (1225); 30790 (1085); 28520 (837); 25615 (630). The d–d-transitions at 20541, 16255 cm^{-1} are visualized with increasing concentration of complex to 10^{-1} mol L^{-1}.

2.3.2. [Fe(H_2L)$_2$]NO_3 complex (**II**)

50.5 mg of the Fe$(NO_3)_3$·9H_2O (0.125 mmol) were dissolved in 15 mL of EtOH. To the resulting solution was added a *HPMHPCTA* solution (58.7 mg, 0.250 mmol in 15 mL of EtOH) under constant stirring. The formed solution was stirred for 15 min, after which it was left for crystallization in the dark. After a day, black crystals formed, which were filtered out and washed with alcohol and diethyl ether.

Dec.*t*. > 230 °C. Yield 0.049 g (67%). *Anal*. Calc. for $C_{22}H_{24}N_7O_5S_2$-Fe: C, 45.06; H, 4.12; N, 16.72; S, 10.94. Found: C, 44.95; H, 4.18; N, 16.77; S, 10.88%.

IR data, ν, cm^{-1}: 3624 broadened absorption band of intermolecular hydrogen bond; 3465, intramolecular hydrogen bond; 3279, ν(NH); 3062, ν(=CH); 3004, asymmetric vibrations $\nu(CH_2)_{allyl}$; 2935, ν(CH); 1660, ν(—C=C—)$_{allyl}$; 1595 ν(C=N); 1534, in-plane deformation vibrations δ(NH—CS—NH); 1465, 1433, phenolic ring vibrations ν(PhH); 1380 ν(CS); 1350, ν(—C—N—); 1309, (NO_3^-) vibrations; 1202 $\nu(C{-}O)_{Ph}$; 1147, ν(NH—CS—NH); 1032, 987, ν(N—N); 942, 907 in-plane deformation vibrations δ(CH); 810, 745, out-of-plane deformation vibrations δ(CH); broadened 592, 464 deformation vibrations $\delta(CH)_{allyl}$, 415, ν(Fe—N); 277, ν(Fe—S).

UV–Vis data, ν, cm^{-1} (EtOH): 39550 (1240); 33923 (700); 32770 (670); 30105 (585); 28550 (473); 26160 (250); 24060 (127).

2.3.3. [Co(H_2L)$_2$]Cl complex (**III**)

36.4 mg of Co$(NO_3)_2$·6H_2O (0.125 mmol) were dissolved in 20 mL of EtOH. To the resulting solution were added 2 mL of 2 M HCl and 20 mL of an ethanol solution of *HPMHPCTA* (58.7 mg, 0.250 mmol) under constant stirring. The formed solution was boiled for 15 min, after which it was left for crystallization. After four days, black-brown needle crystals formed, which were filtered off and washed with ethanol and diethyl ether.

Dec.*t*. > 250 °C. Yield 0.045 g (64%). *Anal*. Calc. for $C_{22}H_{25}N_6O_2S_2$ CoCl: C, 46.85; H, 4.47; N, 14.90; S, 11.37; Cl, 6.29. Found: C, 46.69; H, 4.52; N, 15.01; S, 11.31; Cl, 6.37%.

IR data, ν, cm^{-1}: 3624 broadened absorption band of intermolecular hydrogen bond; 3447, intramolecular hydrogen bond; 3205, ν(NH); 3020, ν(=CH); 3012, asymmetric vibrations $\nu(CH_2)_{allyl}$; 2912, 2785 ν(CH); 1658, ν(—C=C—)$_{allyl}$; 1597 ν(C=N); 1531, in-plane deformation vibrations δ(NH—CS—NH); 1438, 1412, phenolic ring vibrations ν(PhH); 1380 ν(CS); 1340, ν(—C—N—); 1200 $\nu(C{-}O)_{Ph}$; 1153, ν(NH—CS—NH); 1032, 990, ν(N—N); 900 in-plane deformation vibrations δ(CH); 804, 735, out-of-plane deformation vibrations δ(CH); broadened 664, 571, 462 deformation vibrations $\delta(CH)_{allyl}$, 360, ν(Co—N); 275 ν(Co—S).

UV–Vis data, ν, cm^{-1} (EtOH): 39550 (1240); 33700 (1095); 32750 (1095); 29800 (950); 28550 (820); 24272 (335). The d–d-transitions at 19440, 15050 cm^{-1} are visualized with increasing concentration of complex to 10^{-1} mol L^{-1}.

^{1}H NMR data, δ, ppm (DMSO-d_6): 8.88 br. m (2H, N^{3}H); 8.46 s (2H, 2C^{7}H); 7.30 d (2H, J = 7.2 Hz, 2C$^5H_{Ar}$); 7.05 t (2H, J = 8.0 Hz, 2C$^3H_{Ar}$); 6.64 d (2H, J = 8.8 Hz, 2C$^2H_{Ar}$); 6.48 t (2H, J = 7.2 Hz, 2C$^4H_{Ar}$); 5.78–5.88 m (2H, 2C^{10}H); 5.12–5.22 dd (4H, J = 17.2 Hz, J = 10 Hz, 2C$^{11}H_2$); 4.00 m (4H, 2C$^9H_2$).

2.3.4. [Ni(HL)Py] complex (**IV**)

72.8 mg of Ni$(NO_3)_2$·6H_2O weighing (0.250 mmol) were dissolved in 10 mL of EtOH. To the resulting solution were added 0.5 mL of pyridine and a solution of *HPMHPCTA* (58.7 mg, 0.250 mmol in 10 mL of EtOH). The resulting orange solution was carefully evaporated with stirring to reduce the amount of three times. Then were added 20 mL of chloroform and 20 mL of water.

The resulting mixture was extracted, after which the complex goes into the chloroform layer. Resulting solution was washed by separating funnel with two portions (30 mL) of water. The chloroform solution was dried with two grams of anhydrous Na_2SO_4, after which it was filtered and left to evaporate slowly. The red needle-shaped crystals began to form after 2–3 days. The product yield was 91% after complete evaporation of the solvent.

Dec.*t.* > 130 °C. Yield 0.053 g (95%). *Anal.* Calc. for $C_{16}H_{16}N_4NiOS$: C, 51.79; H, 4.35; N, 15.10; S, 8.64. Found: C, 51.65; H, 4.37; N, 15.00; S, 8.48%.

IR data, ν, cm^{-1}: 3637 broadened absorption band of intermolecular hydrogen bond; 3452, 3380 intramolecular hydrogen bond; 3221 $\nu(N^3H)$; 3090 $\nu(=CH)$; asymmetric vibrations $\nu(CH_2)_{allyl}$ and $\nu(CH)_{Py}$; 2972 symmetric vibrations $\nu(CH_2)_{allyl}$; 2883 $\nu(CH)$; 1656, 1634 $\nu(—C=C—)_{allyl}$; 1600 $\nu(C=N)$; 1560, 1535 in-plane deformation vibrations $\delta(—N—CS—N—)$; 1468, 1444 Ph and Py rings vibrations $\nu(PhH)$; 1380 $\delta(CH)$; 1340, 1320 $\nu(—C—N—)$; 1247 $\nu(C—S)$; 1203 $\nu(C—O)_{Ph}$; 1152 $\nu(—N—CS—N—)$; 1028, 992, $\nu(N—N)$; 941, 929, 912 in-plane deformation vibrations $\delta(CH)$; 844, 824, 757, out-of-plane deformation vibrations $\delta(CH)$; broadened 687, 627, 588, 488 deformation vibrations $\delta(CH)_{allyl}$, 357, $\nu(Ni—N)$; 286 $\nu(Ni—S)$.

UV–Vis data, ν, cm^{-1} (EtOH): 40655 (2447); 34745 (1187); 32572 (973); 27470 (1000); 24363 (782), 20917 (100).

^1H NMR data, δ, ppm (DMSO-d_6): 8.85 br. s (2H, N^3H, C^7H) 7.97 m (2H, $C^{12,16}H_{Py}$); 7.52 m (2H, $C^{14,13}H_{Py}$); 7.35 d (1H, J = 8.0 Hz, C^5H_{Ar}); 7.13 m (2H, $C^{3,15}H_{Ar,Py}$); 6.67 d (1H, J = 8.4 Hz, C^2H_{Ar}); 6.57 t (1H, J = 7.2 Hz, C^4H_{Ar}); 5.88–5.82 m (1H, $C^{10}H$); 5.16 d (1H, J = 17.2, Hz, $C^{11}H_2$); 5.06 d (1H, J = 10 Hz, $C^{11}H_2$); 3.74 m (2H, C^9H_2).

^{13}C NMR data, δ, ppm (DMSO-d_6): 168.93 (C8), 161.03 (C1), 151.95 (C7), 151.69 C(10), 138.95 C(4), 135.69 (C12, 16), 132.22 C(3, 5), 132.03 (C14), 119.34 C(2) 118.99 (C6), 115.54 (C11), 114.91 (C13, 15), 47.52 (C9).

3. Results and discussion

The complexation reactions were carried out according to Scheme 1. As a starting salt in the synthesis of the complex **I** we used $CuCl_2{\cdot}2H_2O$ to avoid the formation of reaction by-products. Our experience has shown that in some reaction conditions the interaction of oxygen-containing salts of copper with sulfur-containing ligands like HPMHPCTA leads to their hydrolysis to carbamides and release of elemental sulfur. Therefore, the selection of copper salts for the synthesis of complexes requires caution. As a result, the interaction between ethanol solutions of $CuCl_2{\cdot}2H_2O$ and *HPMHPCTA* leads to the formation of the complex **I**. The monodeprotonated thione form of ligand molecule is coordinated to the metal ion in a tridentate manner to form five- and six-membered metal chelate rings. Vacant coordination site of the Cu(II) occupied by chloride anion (Scheme 1). The Cu^{2+} ion forms a square-planar

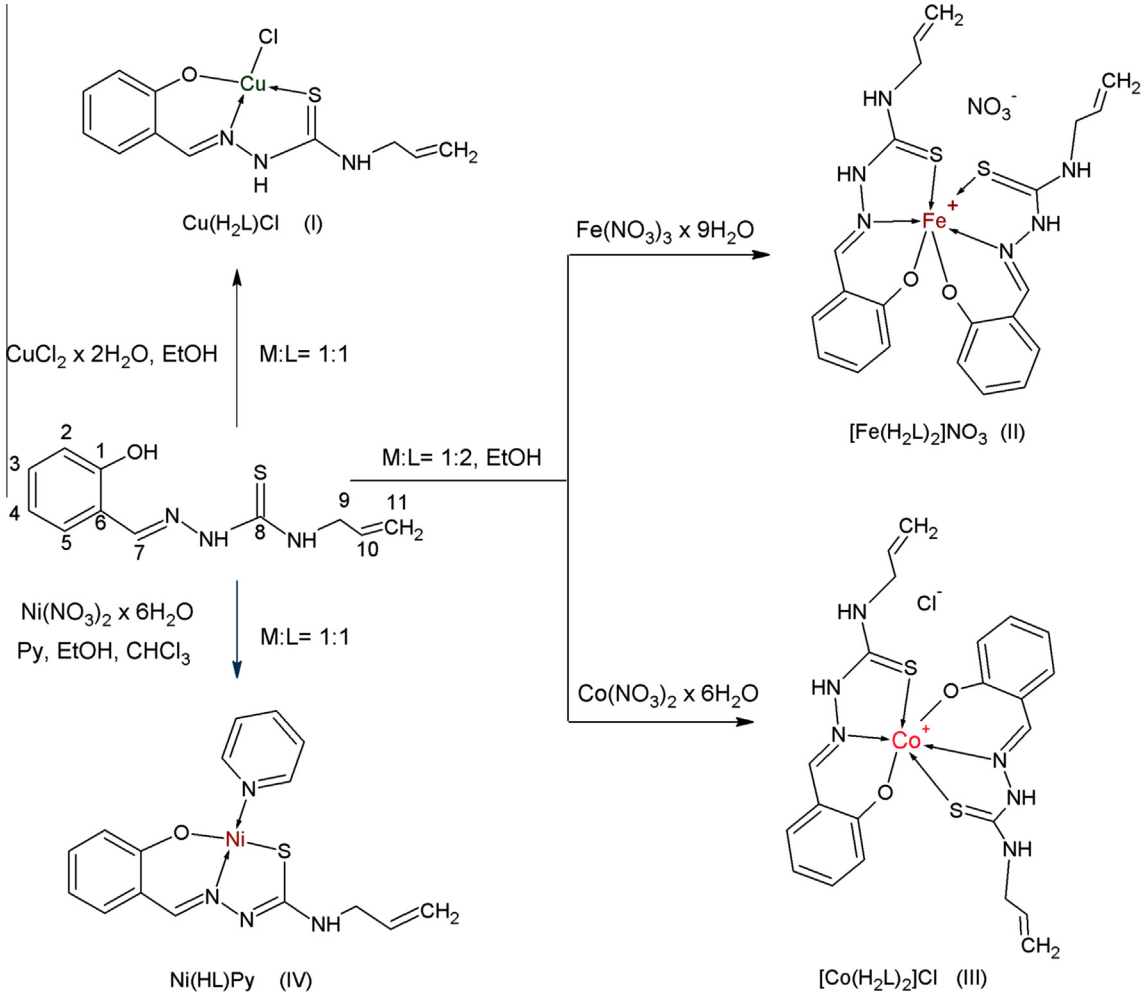

Scheme 1. The scheme of synthesis of complexes **I**–**IV**.

coordination polyhedron, at whose vertices O, N, S, Cl heteroatoms are located.

Using the component ratio M:L = 1:2, Fe(III) and Co(III) complexes **II**, **III** with coordination of two *HPMHPCTA* molecules in the thione tautomeric form have been isolated in the crystalline form.

The presence of outer-anions in the complexes **III** indicates a trivalent state of the central metal ion. Both ligand molecules are coordinated in monodeprotonated form similarly to complex **II** as shown in the synthesis scheme. In this case, in contrast to compound **II**, complex **III** is diamagnetic, which allowed us to study its ^{1}H NMR spectrum, described in Section 3.1.4. To slowdown the complex formation and isolation of crystalline product **III**, a solution of 2 M HCl was added to reaction mixture. Crystals begin to grow roughly on the 4th–5th day with slow evaporation of the solvent. Without the presence of acid, the reaction proceeds rapidly with a formation of fine crystalline product.

To ensure transform to a thiol form of the ligand followed by formation of square-planar complex **IV**, reaction is carried out with the addition of pyridine, as this increases the pH of the medium. Besides, pyridine acts as a heteroligand. Increasing pH by adding a solution of KOH leads to form a mixture of products, including by-products, which does not allow the isolation of the desired complex in a pure solid state. Stable square-planar nickel complexes have been obtained only with pyridine.

The location of nitrate and chloride anions in the outer coordination sphere of the complexes **II**, **III** gives them ionic character, which contributes to their water solubility at room temperature. Besides, the complexes are soluble in ethanol, DMF, DMSO.

3.1. Spectroscopic characterization

3.1.1. IR spectra

The formation of the complexes **I**–**IV** results in the deprotonation of the (OH) group, which leads to the absence of the absorption bands (ABs) ν(OH) in the spectra of these complexes. The ABs of ν(NH) in the spectra of the complexes are shifted by $\Delta\nu$ = 90–114 cm^{-1} to the high-frequency region in comparison with the spectrum of uncoordinated ligand. The AB at 3221 cm^{-1} in the spectrum of the complex **IV** corresponds to ν(N^{3}H), which leads to shift of $\Delta\nu$(NH) only by 54 cm^{-1}. The ABs at 3100, 3090, 3004, 2972, 2943 cm^{-1} correspond to asymmetric and symmetric (C—H) bond vibrations of the allyl fragment. The doublet band at 1620, 1600 cm^{-1}, corresponds to stretching vibrations of $(-C{=}C-)_{allyl}$ bond and (C=N) azomethine group. In the spectra of the complexes **I**–**III**, the ABs of ν(C=N) are shifted to a low-frequency by $\Delta\nu$ = 20–34 cm^{-1}, and the ABs of ν(C=S) shift by $\Delta\nu$ = 30–50 cm^{-1} to the high frequency region, indicating these groups to be involved in coordination to the metal ion. In contrast, the AB of ν(C=S) in the spectrum of **IV** is absent because HPMHPCTA exists in thiol tautomeric form, which leads to the presence in the spectrum a new AB at 1247 cm^{-1}, corresponding to ν(C—S). Besides, in the IR spectra of the complex **II** there is a broadened intense AB at 1309 cm^{-1} corresponding to (NO_3^-) vibrations.

In the low-frequency region of the spectra of the complexes **I**–**IV** the ABs of ν(M—N) at 415–342 and ν(M—S) at 277–280 cm^{-1} can be recognized. In addition the band ν(Cu—Cl) at 304 cm^{-1} is characteristic of complex **I**. The bond vibrations ν(M—O) in the IR spectra of the complexes cannot be identified because of their overlapping with $\delta(CH)_{allyl}$ or with out-of-plane deformation vibrations $\delta(CH)_{Ar}$ of aromatic ring.

3.1.2. UV–Vis spectra

In the spectra of the complexes **I**–**III**, a shift of the ABs to the low frequency region in comparison with free HPMHPCTA is observed (Fig. S1a). The charge-transfer bands (CTBs) of the aromatic ring undergo the strongest low-frequency shift ($\Delta\nu_{(\pi\rightarrow\pi*)Ph}$ = 905–1680 cm^{-1}). The ABs of $\pi\rightarrow\pi^*$ and $n\rightarrow\pi^*$ of the azomethine and thioureide groups shift by $\Delta\nu$ = 107–445 and 120–200 cm^{-1} respectively, indicating the above functional groups to be involved in coordination to the metal ion. The expected ligand-to-metal charge-transfer band (LMCTBs) [S → M] in the complexes **I**–**III** observed at 25 615 cm^{-1} (**I**), 26 160 cm^{-1} (**II**) and 24 272 cm^{-1} (**III**). After increasing the concentration of the complexes to 0.1 M, the bands of d–d transitions in the metal ion at 20 541, 16 255 cm^{-1} (**I**), 24 060 cm^{-1} (**II**), 19 440, 15 050 cm^{-1} (**III**) are visualized in the spectrum (Fig. S1b).

Unlike the complexes **I**–**III**, UV–Vis spectrum of complex **IV** differs significantly. The coordinated thiol tautomeric form of HPMHPCTA leads to the shift of band responsible for $\pi\rightarrow\pi^*$, $n\rightarrow\pi^*$ (C=N) by $\Delta\nu$ = 2530 cm^{-1} to the low frequency region. Coordination pyridine molecules in this complex leads to a AB responsible for $\pi\rightarrow\pi^*$ of $(C{=}N)_{Py}$ at 34 745 cm^{-1}, Fig 1*a*. The ABs of $\pi\rightarrow\pi^*$ (C=C) of aromatic and pyridine rings are combined into a broadened single AB at 40 655 cm^{-1}. The LMCT band of complex **IV** is appearing at 24 362 cm^{-1}. The d–d transitions are visualized at 20 917 cm^{-1}.

The plotting of saturation curves (Fig. S2a–c) showed that the interaction of Cu^{2+}, Fe^{3+} and Co^{2+} ions with *HPMHPCTA* in ethanol solutions leads to the formation of complexes at the component ratios M:L = 1:1 and 1:2. The curves have the best-defined plateau at the component rations M:L = 1:1 (for the Cu(II) complex) and M:L = 1:2 (for the Fe(III) and Co(III) complexes). This shape of the saturation curves indicates indirectly that the complexes have a fairly high stability. This was confirmed subsequently after the calculation of the stability constants ($K_s = 1.12\times10^6$, 9.14×10^7, 7.95×10^8) of the complexes **I**–**III** by the equilibrium displacement method [41–44].

3.1.3. XPS and MALDI-mass spectra

Observations of outer-ions (NO_3^- and Cl^-) in the complexes **II**, **III** prompt us to study N1s and Cl2p binding energies in X-ray photoelectron spectroscopy (XPS) of these complexes (Fig. 1*a*, *b*). Upon decomposition N1s line obtained three components with the values of the binding energy N1s 399.2, 399.9, 400.7 eV (complex **II**) and 398.7, 400.0, 400.86 eV (complex **III**), which is due to three states nonequivalent nitrogen atoms N^{1}H, N^{2}H and —N^3=. However, the N1s lines of **III** and **II** are differ that is the presence of **II** additional peaks at 404.7, 406.55 (**II**) due NO_3^- located in the outer sphere of the complexes [45,46] (Fig. 1b). The value of Cl2p binding energy of complex **III** is 197.5 eV, which correspond to outer-location of Cl^- ion.

The ion exchange and redox processes occur under the conditions of MALDI mass spectrum. Often, this makes it difficult determination of the molecular ion of complexes containing outer-ions. Therefore, we used MALDI-mass spectroscopy for the study of complex **III**, in which the central metal ion changed its valence. Analysis of MALDI-mass spectra of complex **III** showed the presence of peak at 526.57 *m*/*z*, which correspond to molecular ion $C_{22}H_{24}N_6CoO_2S_2$ (Fig. S3). Thus, the outer-chlorine anion was not identified under the conditions of the mass spectra.

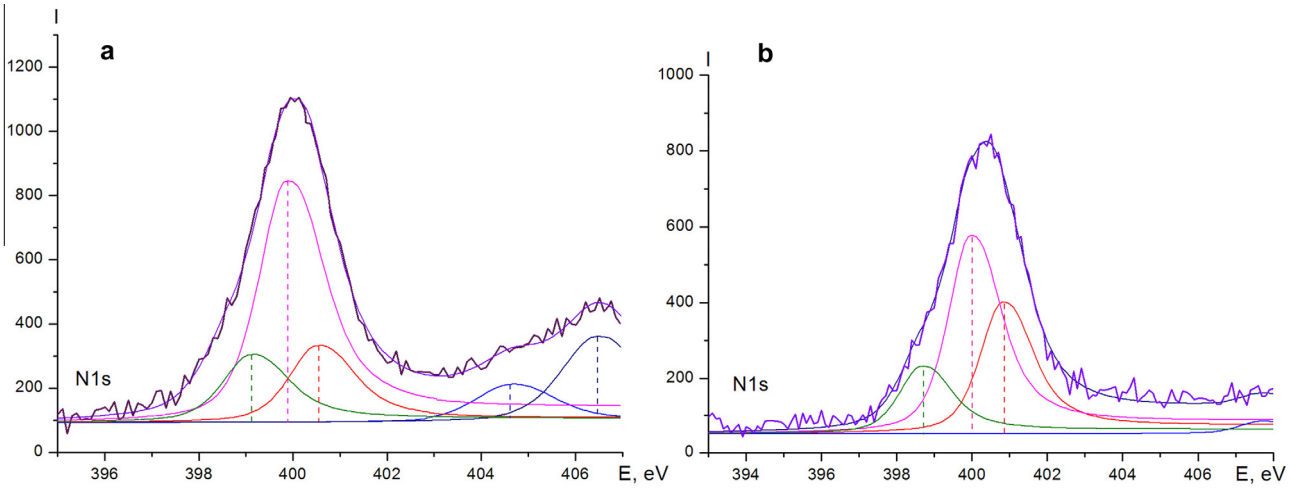

Fig. 1. N1s lines in XPS spectrum of complexes **II** (a) and **III** (b).

3.1.4. ^{1}H and ^{13}C NMR spectra

The character of proton signals of the ^{1}H NMR spectra of complex (**III**) indicates its diamagnetic state (Fig. S4). The absence of the proton signal of OH group indicates the deprotonation of the ligand molecules. Besides, singlets of $N^{3}H$, $C^{7}H$ and doublet of $C^{5}H_{Ar}$ are shifted downfield by $\Delta\delta$ = +0.26, +0.06, +0.67 ppm respectively, whereas the signals of $C^{3,2,4}H_{Ar}$ are shifted upfield by $\Delta\delta$ = −0.18, −0.25, −0.36 ppm in comparison with free HPMHPCTA [34].

Analysis of the ^{1}H NMR spectra of complex **IV** showed that the $N^{3}H$ proton signal of chelate coordinated ligand molecules is shifted downfield by $\Delta\delta_{(NH)}$ = +0.4 ppm. Additionally, this signal overlapped with the signal of the $=C^{7}H$ proton forming broad singlet at 8.5 ppm. Other proton signals at C9, C10, C11, C2, C3, C4, C5, are shifted upfield by $\Delta\delta$ = 0.49, 0.08, 0.12, 0.22, 0.1, 0.27, 0.62 ppm. It is due to coordination of the ligand molecules to the metal ion with the formation of metal chelate rings through the nitrogen of (C=N), sulfur of (C—S) and oxygen of the fragment (Ar—O). The absence of $N^{2}H$ proton signal in the spectrum can be explained by thiolic form of the ligand.

In the ^{13}C NMR spectrum of complexes **IV**, carbon signals C8 ($\Delta\delta$ = −8.07), C1 ($\Delta\delta$ = +4.71), C7 ($\Delta\delta$ = +12.83) directly related to the sulfur, oxygen and nitrogen involved in the formation of coordination bonds Ni—S, Ni—O and Ni—N undergo the most significant shift. The slight downfield and upfield shift of other carbon signals of coordinated HPMHPCTA molecule is also observed. The signals at 135.69, 132.03 and 114.91 ppm correspond to pyridine carbons.

3.2. Crystal structures

The complex **I** in crystal phase exists as a monohydrate (Fig. 2). The Cu1 atom has planar–square coordination. It forms bonds with the S1, N1 and O1 of organic ligand and the chloride anion. Length of the O1—C1 bond (1.320(3) Å) and absence of the hydrogen atom at the O1 clearly demonstrates anionic character of this oxygen atom. All non-hydrogen atoms of organic anion except allyl group are co-planar within 0.03 Å. The allyl substituent at the N3 atom adopts orthogonal orientation with respect to this plane (the C8—N3—C9—C10 torsion angle is 87.7(3)°) and its terminal C10—C11 double bond is synperiplanar to the N3—C9 bond (the N3—C9—C10—C11 torsion angle is −4.2(3)°).

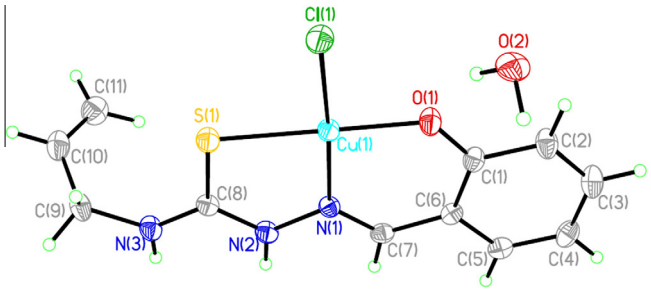

Fig. 2. The molecular structure of monohydrate of complex **I**. Thermal ellipsoids are shown at 30% probability level.

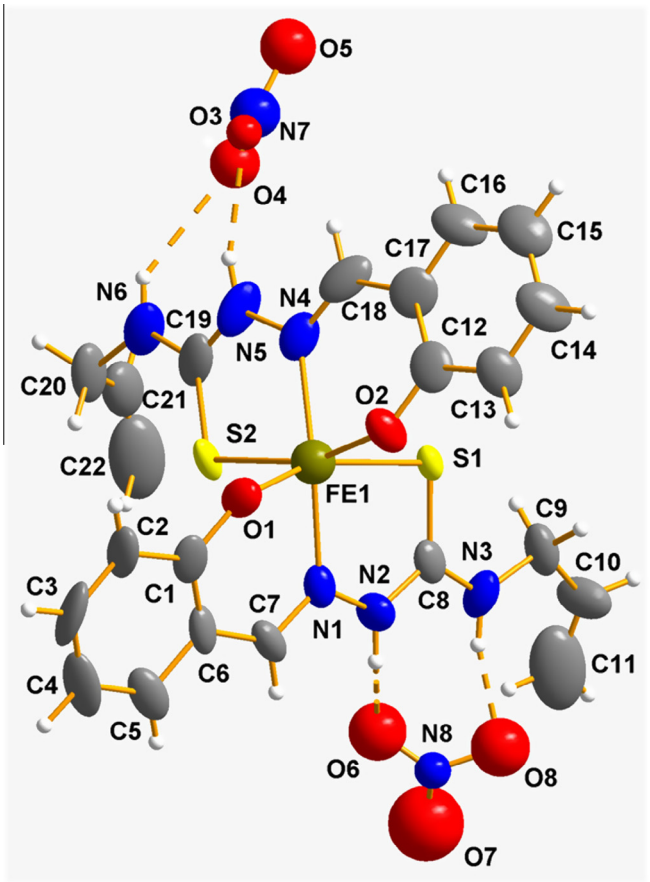

Fig. 3. The molecular structure of complex **II** with labeling scheme. Thermal ellipsoids are shown with 50% probability. Two position of disordered nitrate anion is shown.

In the crystal phase complexes **I** form stacks along [1 0 0] crystallographic direction with head-to-tail arrangement of molecules due to stacking interactions between planar fragments of ligands (the distances between planes of neighboring ligands are 3.34 Å and 3.24 Å), Fig. S5. Complexes of neighboring stacks are bonded by the hydrogen bonds with water molecules: O2—H···O1 (H···O 1.91 Å, O—H···O 158°), O2—H···Cl1′ (1 − *x*, 1 − *y*, 1 − *z*) (H···Cl 2.27 Å, O—H···Cl 164°), O2···H—N2′ (*x*, −1 + *y*, *z*) (O···H 1.87 Å, O···H—N 177°), Tables S1 and S2.

The complex **II** is crystallized in a triclinic symmetry. The asymmetric unit contains one molecule of the complex and nitrate counter anion, connected to the main moiety by H-bonds. The central ion of Fe has a strongly distorted octahedral coordination environment that consists of two oxygens, two nitrogens and two sulfurs from two different ligand molecules. The adjacent angles around the Fe are in a wide range of 78.4(3)–113.6(3)°. The Fe—S bond lengths are in range 2.465–2.490(3), which is not consistent with all other complexes described here [47], Table S3. The ligand molecules are coordinated tridentately in the same way like in complex **IV**. The position of the nitrate anion in the crystal structure suggests the presence of the hydrogen atoms on both carbothioamide nitrogens (Fig. 3). In the crystal structure, the molecules are interacted by hydrogen bonds (Table S4) and weak Van der Waals intermolecular interactions.

Molecular structure of complex **III** is very similar to complex **II** (Fig. 4). The cobalt atom is coordinated by two anionic ligands with different orientations of the allyl substituents (the C8—N3—C9—C10 and C19—N6—C20—C21 torsion angles are −157.3(5)° and −85.3(6)°, respectively), Table S5. However, these two complexes significantly differ in the crystal structure. This allows determining positions of additional chloride anion and solvent molecule. The central carbon atom of the solvating ethanol molecule is disordered over two positions with equal population. Such relatively minor disorder of solvent, probably, is caused by the formation of the O3—H···O2 hydrogen bond to complex cation (O···H 2.08 Å, O—H···O 156°).

Complexes **III** in the crystal phase form infinite columns along [1 0 0] crystallographic axis stabilized by the stacking interactions between the same ligands of neighboring complexes located in head-to-tail manner, Fig. S6. The shortest distances between atoms of stacked ligands are 3.18 Å and 3.24 Å for two different ligands. Neighboring columns are bonded by the N—H···Cl hydrogen bonds: N5—H···Cl1 (H···Cl 2.15 Å, N—H···Cl 171°), N6—H···Cl1 (H···Cl 2.40 Å, N—H···Cl 140°), Table S6.

In the complex **IV** the nickel ion displays a slightly distorted square-planar coordination geometry formed by phenyl oxygen O(1), azomethine nitrogen N(1), thioamide sulfur S(1) and pyridine nitrogen N(4), Fig. 5. The adjacent angles near the nickel ion are in range 83.0(4)–96.27(6)° (Table S7).

The organic ligand coordinates to central atom like in the all previous cases forming five- and six-membered planar metallarings. The mean deviation from least-square planes Ni1—N1—N2—C8—S1 and Ni1—O1—C1—C6—C7—N1 are 0.0311 and 0.0239 Å. Both metallarings are co-planar with dihedral angle of 4.9(1)°. The both positions of coordinated pyridine molecules are not co-planar with the main moiety creating the dihedral angles of 61.6(3)° and 49.9(3)°. Values of the C1—O1(1.309(2) Å), C(8)—S(1) and N(2)—C(8) (1.7450(18) Å and 1.309(2) Å, respectively) bond lengths indicates that HPMHPCTA ligand exist as phenolic anion in thiolic tautomeric form. The analysis of the crystal structure of **IV** reveals the formation of macrocyclic dimmers by intermolecular N—H···N hydrogen bonds. (Fig. 5), Table S8.

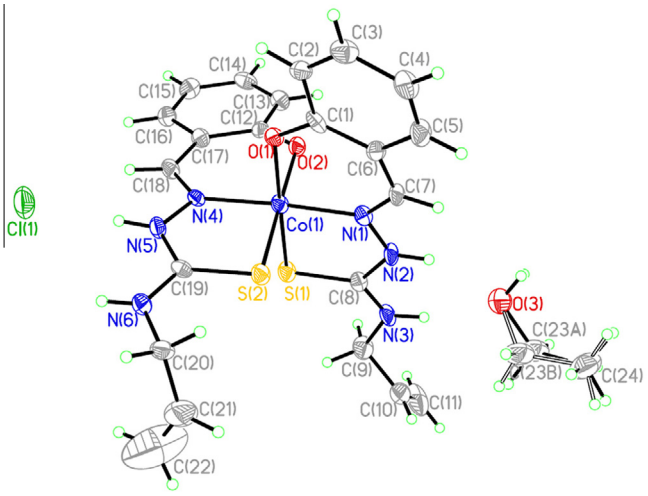

Fig. 4. The molecular structure of complex **III**. The ethanol molecules is disordered within two orientations.

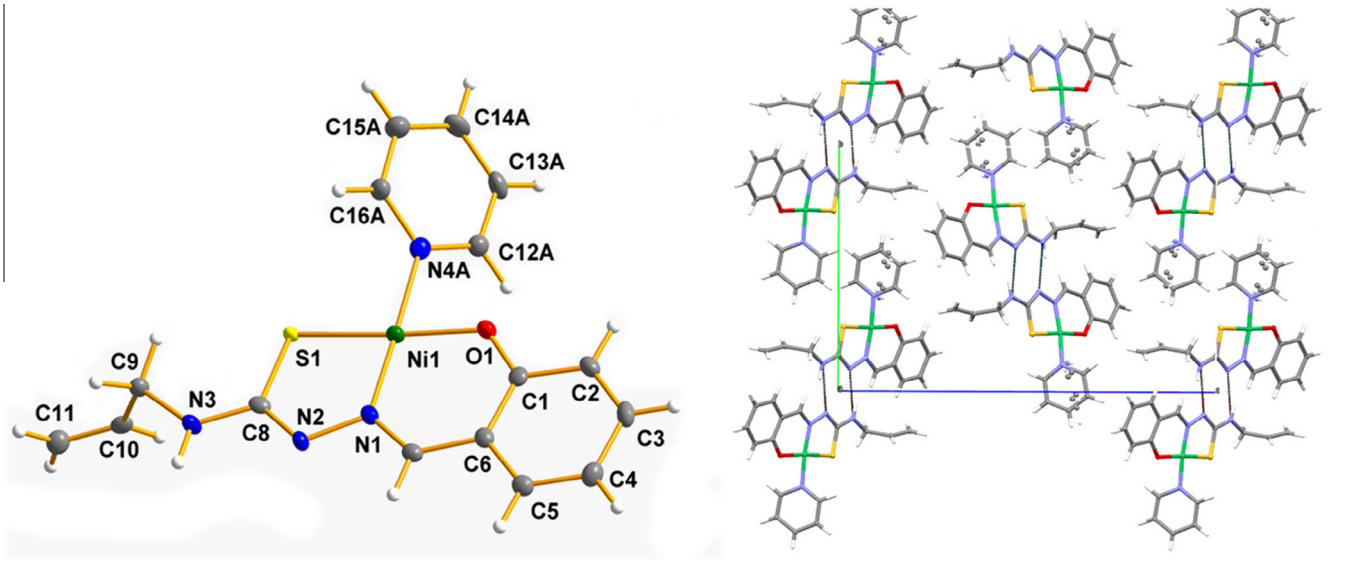

Fig. 5. Molecular structure of **IV** with labeling scheme. Thermal ellipsoids are shown with 50% probability. The second (B) position of disordered pyridine ring is omitted for clarity.

4. Conclusions

Four novel complex compounds with composition $[Cu(H_2L)Cl]$ (**I**), $[Fe(H_2L)_2]NO_3$ (**II**), $[Co(H_2L)_2]Cl$ (**III**) and [Ni(HL)Py] (**IV**) (L-HPMHPCTA) have been synthesized and characterized by X-ray diffraction, IR, UV–Vis and ^1H, ^{13}C NMR spectroscopy. It was proved that HPMHPCTA in all cases coordinates in a tridentate manner being in the thione (complexes **I–III**) or thiol (complex **IV**) tautomeric form depending on synthesis conditions. This coordination contributes to lowering the frequency of the main characteristic absorption bands in UV–Vis and IR spectrum. The presence of outer NO_3^- and Cl^- anions in the complexes **II**, **III** has been described additionally by the XPS spectrum. The ^1H, ^{13}C NMR spectral characteristics of the complexes **III**, **IV** have been described. The calculated stability constant of the complexes **I–III** indicate their relatively high stability in solution.

Acknowledgements

The authors are thankful to Dr. Olga Severinovskaya, Institute of Surface Chemistry NAS of Ukraine for the measuring of MALDI mass spectrum.

Appendix A. Supplementary material

The UV–Vis, ^1H NMR and MALDI-mass spectra are given as Supplementary data in Figs. S1−S4. CCDC 979142, 998510, 979144 and 998509 for complexes **I**, **II**, **III** and **IV**, respectively. These data can be obtained free of charge from The Cambridge Crystallographic Data Centre via www.ccdc.cam.ac.uk/data_request/cif. Selected bond lengths, angles and Hydrogen bonds for the complexes **I–IV** and packing of complexes (**I**), (**III**) are given as Supplementary data in Tables S1−S8 and Figs. S5, S6. Supplementary data associated with this article can be found, in the online version, at http://dx.doi.org/10.1016/j.ica.2014.08.056.

References

[1] T.S. Lobana, R. Sharma, R. Sharma, S. Khana, Coord. Chem. Rev. 253 (2009) 977.
[2] J.S. Casas, M.S. García-Tasende, J. Sordo, Coord. Chem. Rev. 209 (2000) 197.
[3] S. Chandra, P. Ballabh, Int. J. Pharm. Sci. Res. 4 (2013) 2393.
[4] A. Castiñeiras, R. Pedrido, Dalton Trans. 39 (2010) 3572.
[5] Y. Yu, D.S. Kalinowski, Z. Kovacevic, A.R. Siafakas, P.J. Jansson, C. Stefani, D.B. Lovejoy, P.C. Sharpe, P.V. Bernhardt, D.R. Richardson, J. Med. Chem. 52 (2009) 5271.
[6] S. Anitha, J. Karthikeyan, A.N. Shetty, Indian J. Chem. 52A (2013) 45.
[7] P.J. Jansson, P.C. Sharpe, P.V. Bernhardt, D.R. Richardson, J. Med. Chem. 53 (2010) 5759.
[8] M. Leigh, D.J. Raines, C.E. Castillo, A.K. Duhme-Klair, ChemMedChem 6 (2011) 1107.
[9] E.C. Moore, M.S. Zedeck, K.C. Agrawal, A.C. Sartorelli, Biochemistry 9 (1970) 4492.
[10] L.-H. Chen, Y.-H. Hu, W. Song, K.-K. Song, X. Liu, Y.-L. Jia, J.-X. Zhuang, Q.-X. Chen, J. Agric. Food Chem. 60 (2012) 1542.
[11] M.-H. Yang, C.-M. Chen, Y.-H. Hu, C.-Y. Zheng, Z.-C. Li, L.-L. Ni, L. Sun, Q.-X. Chen, J. Biosci. Bioeng. 115 (2013) 514.
[12] H. Pervez, M.S. Iqbal, M.Y. Tahir, F.U. Nasim, M.I. Choudhary, K.M. Khan, J. Enzyme Inhib. Med. Chem. 23 (2008) 848.
[13] G.B. Kauffman, Coord. Chem. Rev. 63 (1985) 127.
[14] L.P. Zhenga, C.L. Chena, J. Zhoua, M.X. Lia, Y.J. Wua, Z. Naturforsch. 63b (2008) 1257.
[15] K.W. Tan, H.L. Seng, F.S. Lim, S.-C. Cheah, C.H. Ng, K.S. Koo, M.R. Mustafa, S.W. Ng, M.J. Maah, Polyhedron 38 (2012) 275.
[16] P.I.S. Maia, H.H. Nguyen, D. Ponader, A. Hagenbach, S. Bergemann, R. Gust, V.M. Deflon, U. Abram, Inorg. Chem. 51 (2012) 1604.
[17] M.-A. LeBlanc, A. Gonzalez-Sarrías, F.A. Beckford, P.C. Mbarushimana, N.P. Seeram, Int. J. Inorg. Chem. (2011) 8. Article ID 624756.
[18] G. Pelosi, F. Bisceglie, F. Bignami, P. Ronzi, P. Schiavone, M.C. Re, C. Casoli, E. Pilotti, J. Med. Chem. 53 (2010) 8765.
[19] R.M. Tada, T.S. Maheta, M.B. Gondaliya, M.K. Shan, Chem. Sci. Trans. 2 (2013) 135.
[20] S.D. Patila, R.D. Kamblea, S.V. Hesea, A.P. Achayaa, B.S. Dawanea, J.R. Koteb, R.N. Gachhe, Der Pharm. Sin. 4 (2013) 171.
[21] B. Demoro, M. Rossi, F. Caruso, D. Liebowitz, C. Olea-Azar, U. Kemmerling, J.D. Maya, H. Guiset, V. Moreno, C. Pizzo, G. Mahler, L. Otero, D. Gambino, Biol. Trace Elem. Res. 153 (2013) 371.
[22] D. Bahl, F. Athar, M.B.P. Soares, M.S. de Sá, D.R.M. Moreira, R.M. Srivastava, A.C.L. Leite, A. Azam, Bioorg. Med. Chem. 18 (2010) 6857.
[23] S. Sharma, F. Athar, M.R. Maurya, F. Naqvi, A. Azam, Eur. J. Med. Chem. 40 (2005) 557.
[24] S. Suganya, D. Udhayakumaria, S. Velmathi, Anal. Methods 5 (2013) 4179.
[25] R.B. Singh, H. Ishii, Crit. Rev. Anal. Chem. 22 (1991) 381.
[26] A.G. Asuero, M. Gonzalez-Balairon, Microchem. J. 25 (1980) 14.
[27] G. Ramanjaneyulu, P.R. Reddy, V.K. Reddy, T.S. Reddy, Open Anal. Chem. J. 2 (2008) 78.
[28] N.M. Modawe, M.A.Z. Eltayeb, Adv. Anal. Chem. 3 (2013) 1.
[29] N.B. Patel, Y.J. Solanki, Int. J. ChemTech Res. 5 (2013) 1545.
[30] A. Mazloomifar, M. Ahadi, Int. J. Sci. Res. Knowledge 1 (2013) 140.
[31] A.S.M. Ali, N.A. Razak, I.A. Rahman, World Appl. Sci. J. 16 (2012) 1040.
[32] S.A. Reddy, K.J. Reddy, S.L. Narayana, Y. Sarala, A.V. Reddy, J. Chin. Chem. Soc. 55 (2008) 326.
[33] S.I. Orysyk, V.V. Bon, O.O. Obolentseva, Yu.L. Zborovskii, V.V. Orysyk, V.I. Pekhnyo, V.I. Staninets, M.V. Vovk, Inorg. Chim. Acta 382 (2012) 127.
[34] S.I. Orysyk, V.V. Bon, O.O. Zholob, V.I. Pekhnyo, V.V. Orysyk, Yu.L. Zborovskii, M.V. Vovk, Polyhedron 51 (2013) 211.
[35] V.V. Bon, Sect. C Cryst. Struct. Commun. 66 (2010) m300.
[36] V.V. Bon, S.I. Orysyk, V.I. Pekhnyo, Russ. J. Coord. Chem. 37 (2011) 149.
[37] Bruker, SAINT, Bruker AXS Inc., Madison, Wisconsin, USA, 2002.
[38] G.M. Sheldrick, SADABS, University of Gottingen, Germany, 2003.
[39] Bruker, SHELXTL, Bruker AXS Inc., Madison, Wisconsin, USA, 2001.
[40] H. Hempel, Chem. Ber. 27 (1894) 625.
[41] J.M. Gardlik, Spectrophotometric determination of stability constants: a study of the complex ions formed from di-n-butyloxadmidine and Ni2+, Co2+, and Cu2+ ions, Spring term, 1974.
[42] L. Nikolova, A. Surleva, T. Nedeltcheva, R. Borissova, J. Univ. Chem. Technol. Metallurgy 46 (2) (2011) 203.
[43] E. Kleszczewska, Pol. J. Environ. Stud. 8 (1999) 313.
[44] E. Norkus, I. Stankevičienė, A. Jagminienė, K. Prušinskas, Chemija 22 (2011) 131.
[45] V.I. Nefedov, Russ. J. Coord. Chem. 1 (1975) 291.
[46] V.I. Nefedov, X-ray Electronic Spectroscopy of the Chemical Compounds, Chemistry, Moscow, 1984.
[47] F.H. Allen, O. Kennard, D.G. Watson, L. Brammer, A.G. Orpen, R. Taylor, J. Chem. Soc., Perkin Trans. 2 (1987) S1.